Journal of Molecular Structure 1050 (2013) 81–87

Contents lists available at ScienceDirect

Journal of Molecular Structure

journal homepage: www.elsevier.com/locate/molstruc

One-pot solvothermal synthesis of novel cobalt salicylaldimine–urea complexes: A new approach to Co_3O_4 nanoparticles

M.Y. Nassar *, T.Y. Mohamed, I.S. Ahmed

Faculty of Science, Chemistry Department, Benha University, Benha 13518, Egypt

HIGHLIGHTS

- We report the in situ solvothermal of three novel Co(II)-1,3bis(salicylaldimine) urea complexes.
- Spinel cobalt oxide nanoparticles were prepared by thermal decomposition.
- The produced Co_3O_4 showed semiconducting characteristics.
- The as-prepared products were characterized using different analytical and spectroscopic tools.

GRAPHICAL ABSTRACT

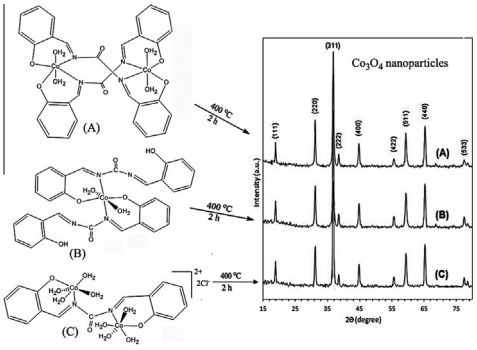

ARTICLE INFO

Article history:
Received 11 April 2013
Accepted 17 July 2013
Available online 22 July 2013

Keywords:
Nano-sized Co_3O_4
Co(II) complexes
Solvothermal synthesis
Thermal analysis
Optical properties

ABSTRACT

Three novel Cobalt salicylaldimine–urea complexes $\{[Co_xL_y(H_2O)_n]Cl_z$; where, L = 1,3-bis(salicylaldehydimine)urea Schiff base; x, $y = 1$ or 2; $n = 2$ or 8; $z = 0$ or 2$\}$ were synthesized by one-pot solvothermal treatment of methanolic solutions of urea, salicylaldehyde, and cobalt chloride at 120 °C for 3 h. Subsequently, normal spinel-type Co_3O_4 nanoparticles, with an average crystallite size in the range 22–38 nm, were easily produced via thermal decomposition of the synthesized complexes at 400 °C for 2 h. The synthesized compounds were characterized by elemental analysis, thermal analysis (TG-DTA/DTG), X-ray powder diffraction (XRD), Fourier transform infrared spectroscopy (FT-IR), UV–Vis spectroscopy, transmission electron microscopy (TEM) and EI mass spectroscopy. Investigation of the optical properties of the produced cobalt oxide, using UV–Vis spectroscopy, confirmed its semiconducting properties by revealing two optical band gabs in the range of 1.42–1.50 and 1.83–1.95 eV.

1. Introduction

Synthesis of metal–organic coordination compounds under hydro-/solvothermal conditions at a relatively low temperatures of 100–200 °C has received much attention not only due to the chance to produce complexes with novel structures and properties, but also the in situ ligand synthesis. However, reports on hydrothermal synthesis of Schiff base coordination complexes including the in situ ligand synthesis are limited [1,2]. Additionally, Schiff base coordination complexes are still of great importance because of their simple preparation, diverse chemical structures, wide applications such as biological modeling, catalysis, molecular magnets and material chemistry [3–8]. Plus, to the best of our knowledge, although urea and salicyladehyde are readily available and inexpensive materials, the hydro/solvothermal in situ synthesis of urea-Schiff-base ligands has not been reported.

On the other hand, using coordination and organometallic compounds as new precursors to produce nano-sized metal oxide particles has been regarded as one of the most convenient and

* Corresponding author. Tel.: +20 1068727555; fax: +20 133222578.
E-mail address: m_y_nassar@yahoo.com (M.Y. Nassar).

0022-2860/$ - see front matter © 2013 Elsevier B.V. All rights reserved.
http://dx.doi.org/10.1016/j.molstruc.2013.07.027

practical routes because it does not only help to avoid special instruments and complicated processes, but also it provides novel structures and good purity for the resultant products [9–12]. Among those nanosized metal oxides, spinel cobalt oxide (Co_3O_4) still plays an important role because of its vast applications in electrochromic devices, solid-state sensors, lithium batteries, and catalysis [13–16]. Although there are several valid routes for synthesis of cobalt oxide nanostructures such as nanocasting method, surfactant template approach, and others, these methods are complicated and/or require long time [17–20]. The numerous methods developed for synthesis of cobalt oxide nanostructures, using the organometallic/coordination compounds as precursors have been considered as one of the most convenient and practical approaches.

In our group, we have been interested in the synthesis of cobalt oxide nanoparticles. As such, we reported on the synthesis of Co_3O_4 nanoparticles through thermal decomposition of cobalt carbonate microspheres prepared by hydrothermal method [21,22]. A major interest at the moment is using a new organometallic or coordination compound for the preparation of metal oxide nanoparticles to control nanocrystal size, shape, and distribution size.

Herein, we reported for the first time, the solvothermal synthesis of some novel Co(II)-1,3bis(salicylaldimine) urea complexes. The complexes were then used as solid precursors to produce pure-phase Co_3O_4 nanoparticles by thermal decomposition at 400 °C for 2 h. The products were characterized by using XRD, TEM, FT-IR, TG/ DTA analysis, Mass spectrometry and UV–Vis spectroscopy. Moreover, the optical characteristics of the produced cobalt oxide nanoparticles were investigated.

2. Experimental

2.1. Materials and reagents

All the chemical reagents used were of analytical grade and were purchased and used as received without further purification: cobalt chloride ($CoCl_2{\cdot}6H_2O$; Sigma–Aldrich), urea ($CO(NH_2)_2$; Fluka), and salicyaldehyde ($C_7H_6O_2$; Sigma–Aldrich).

2.2. Synthesis of precursors

2.2.1. Preparation of $[Co_2L_2(H_2O)_4]$ complex (A)

In a typical solvothermal synthesis, urea (0.60 g, 0.01 mmol), salicylaldhyde (1.526 mL, 0.02 mmol) and cobalt chloride (2.54 g, 0.01 mmol) were dissolved in 60 mL methanol in an Erlenmeyer flask and vigorously stirred for about 10 min for complete dissolution and mixing. The reaction blend was then transferred to a Teflon-lined stainless steel autoclave (capacity 100 mL). The autoclave was closed and kept inside an electric oven at 120 °C for 3 h. After reaction, the product was filtered off, washed with methanol and then dried at 60 °C to give a brown powder (2.3 g, 61%). *Anal.* Cal. For $C_{30}H_{28}Co_2N_4O_{10}$ (MW = 722.43): C, 49.88; H, 3.91; N, 7.76%. Found: C, 49.62; H, 3.65; N, 7.54%.

2.2.2. Preparation of $[CoL_2(H_2O)_2]$ complex (B)

In a similar experiment, urea (1.20 g, 0.02 mmol), salicyaldehyde (3.52 mL, 0.04 mmol), cobalt chloride (2.38 g, 0.01 mmol), and 60 mL methanol were solvothermally treated in an autoclave (capacity 100 mL) at 120 °C for 3 h. The obtained precipitate was collected by filtration, washed with methanol and dried at 60 °C to give yellow–brown powder (3.26 g, 55%). *Anal.* Cal. For $C_{30}H_{26}CoN_4O_8$ (MW = 629.48): C, 57.24; H, 4.16; N, 8.90%. Found: C, 57.11; H, 3.96; N, 8.77%.

2.2.3. Preparation of $[Co_2L(H_2O)_8].2Cl$ complex (C)

A mixture of urea (0.3 g, 0.005 mmol), salicylaldhyde (0.76 mL, 0.01 mmol) and cobalt chloride (2.38 g, 0.01 mmol) was dissolved in 60 mL methanol then transferred into an autoclave (capacity 100 mL) and solvothermally treated at 120 °C for 3 h. The produced precipitate was filtered off, washed with methanol, and dried at 60 °C to give yellow–brown powder (3.06 g, 51%). Elem. Anal. Calc. (Found): C, 31.90(32.20); H, 4.82 (4.74); N, 4.96 (4.89)%.

2.3. Preparation of nano-sized tricobalt tetroxide (Co_3O_4)

The as-prepared Co(II)-1,3bis(salicylaldimine) urea complexes **A**, **B** and **C** were thermally decomposed at 400 °C in an open air

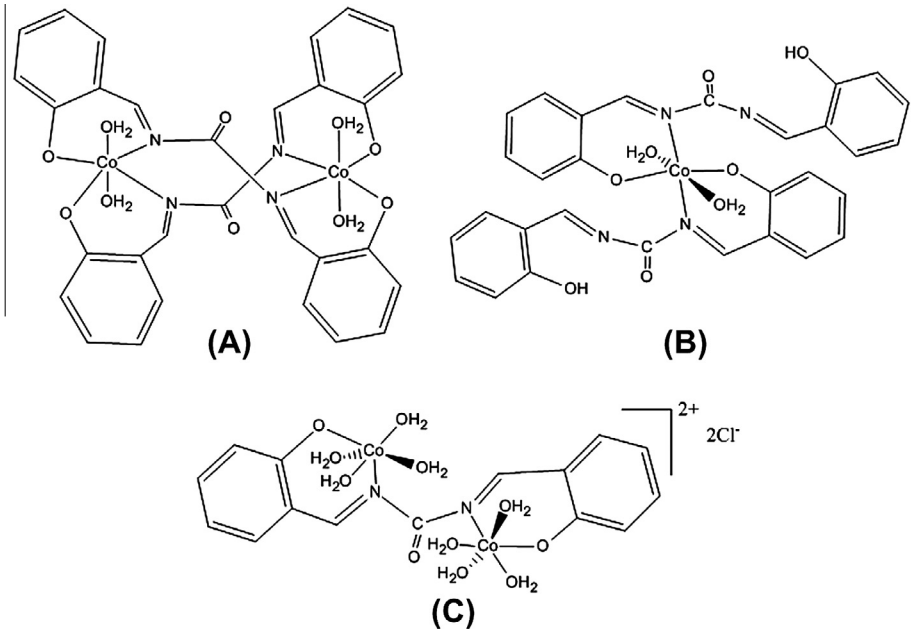

Scheme 1. Proposed structures for the as-prepared Co(II)-1,3bis(salicylaldimine) urea: A, B, and C complexes.

electric furnace for two hours to produce tricobalt tetroxides; A-Co_3O_4, B-Co_3O_4 and C-Co_3O_4, respectively.

2.4. Physical measurements

Elemental analyses were taken using a Perkin–Elmer 2400 CHN elemental analyzer. The infrared spectra (4000–400 cm^{-1}) were recorded as KBr pellets on a Perkin Elmer 550 FTIR spectrometer. Magnetic measurements were carried out at room temperature by Gouy's method using $Hg[Co(SCN)_4]$ as a calibration standard and were corrected for diamagnetism by applying Pascal's constants [23,24]. UV–Vis spectra were recorded on a Jasco UV–Vis spectrophotometer (Jasco; model v530). The thermal analyses were recorded on a Shimadzu DT-30 thermal analyzer from 27 to 700 °C with heating rate 10 °C/min under nitrogen atmosphere. The EI mass spectra were recorded by the EI technique at 70 eV

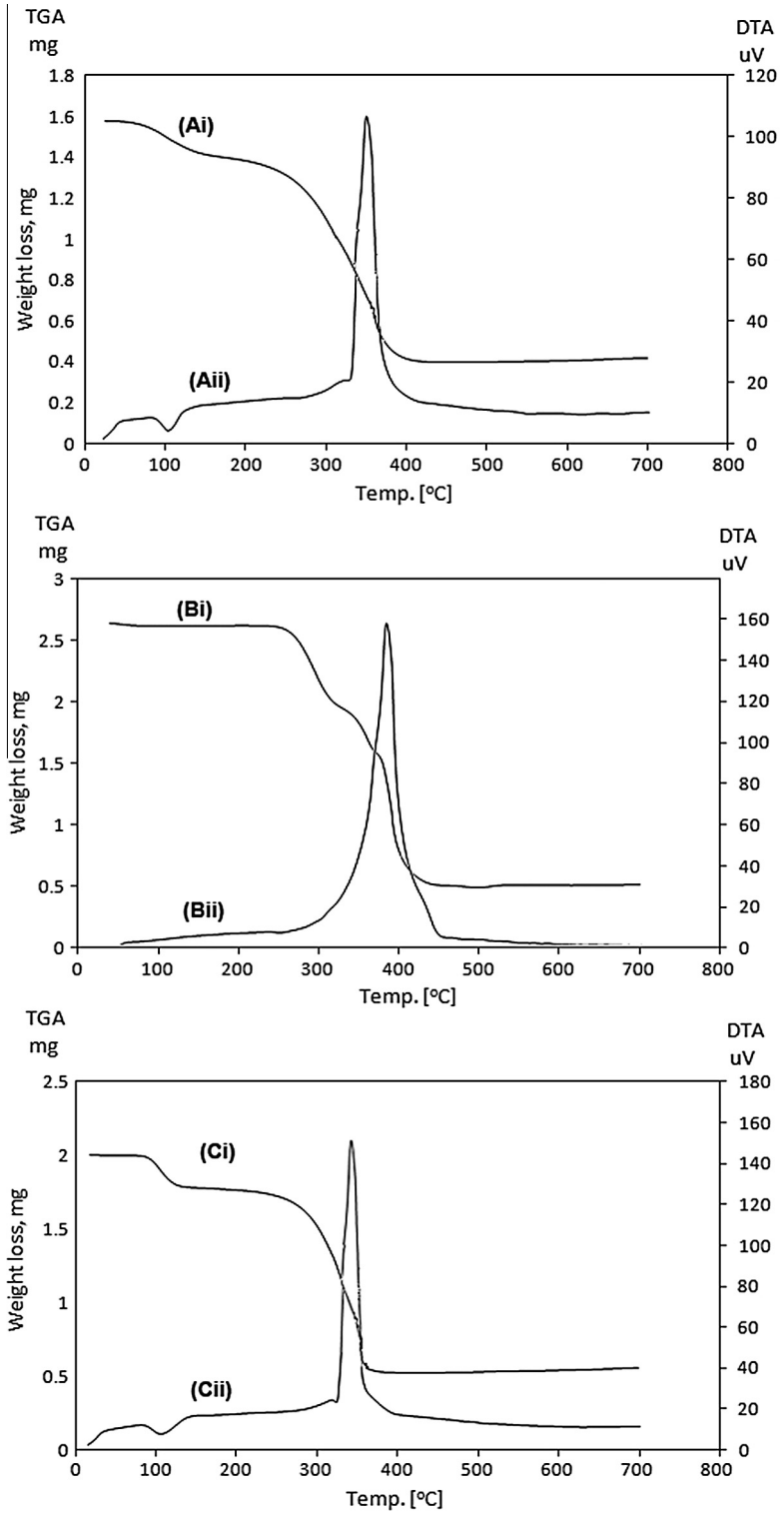

Fig. 1. (A–C) Thermal analyses of the as-prepared Co(II)-1,3bis(salicylaldimine) urea complexes (A, B, and C) in nitrogen atmosphere.

with a Schimadzu-GCMSQP 1000EX quadruple mass spectrometer with electron multiplier detector equipped with a GC–MS data system. The structures and phase compositions of the as-synthesized Co_3O_4 nanoparticles were characterized by powder X-ray diffraction (XRD) using an 18 kW automated diffractometer (Bruker; model D8 advance) with monochromatic Cu Kα radiation (λ 1.54178 Å). The TEM images were taken on a transmission electron microscope (Jeol; model 1200 EX) at an accelerator voltage of 80 kV.

3. Results and discussion

3.1. Solid Co-precursors

3.1.1. Synthesis and characterization

The solid complex precursors (**A, B** and **C**) were synthesized by one-step solvothermal treatment of methanolic solutions of urea, salicyaldehyde, and cobalt chloride in molar ratios (1:2:1), (2:4:1) and (1:2:2) (urea: salicylaldhyde: Co^{2+}, respectively) at 120 °C for 3 h. Characterization of the complexes was carried out by IR, elemental analysis, magnetism, electronic spectra, thermal analysis, UV–Vis spectroscopy and mass spectrometry. The structures of the complexes are presented in Scheme 1. In such, the IR spectra, of **A**, **B** and **C** complexes exhibited a broad band at 3428, 3433 and 3409 cm^{-1}, respectively, corresponding to the frequency vibrations of (OH) group of the coordinating water molecules and/or the uncoordinated OH groups of the 1,3bis(salicylaldimine) urea ligand. The bands appeared at 1650, 1624 and 1650 cm^{-1} are assigned to the stretching vibration of $\nu_{C=O}$ groups for the A, B, and C complexes, respectively. While the frequency bands appeared at 1526, 1532 and 1528.3 cm^{-1} are corresponding to the stretching vibration of $\nu_{C=N}$ groups coordinated with metal ion [25]. For the three complexes, the vibration bands appeared in the range 897–754 cm^{-1} can be assigned to the bending vibration of δ_{OH} group. The stretching frequencies in range 750–740 and 660–566 cm^{-1} are corresponding to ν_{M-N} and ν_{M-O}, respectively. Consequently, the spectra of the complexes showed a good evidence for the synthesis of the solid precursor complexes.

The room temperature magnetic moments of Co(II) complexes (A, B and C) have been found to be 6.06, 4.90, and 6.09 B.M., respectively. The magnetic moment values obtained for **A** and **C** complex indicate that there is an antiferromagnetic interaction occurs between two coordinated Co(II) ions in the complexes with octahedral geometry for each cobalt center [23,26]. However, the magnetic moment value obtained for **B** complex lies within the range expected for octahedral geometry mononuclear cobalt complex [27]. The electronic spectra of Co(II) complexes were similar and revealed four broad and irregular peaks at 37,735, 30,960 and 26,525 cm^{-1}. The first one can be assigned to $\pi \rightarrow \pi^*$ transition in the ligand. The next two may be attributed to ligand-metal charge-transfer (LMCT). Additionally, within the visible range there was a maximum of absorption corresponding to the *d–d* transition for the cobalt complexes appeared at ca. 17,271 cm^{-1}.

The as-prepared complexes were further characterized using mass spectroscopy. Complex **A** showed fragments at m/z = 342, 149, 121, 93, 76 and 58 corresponding to CoOL, $C_8H_5O_2N$, C_7H_6NO, $CoO(H_2O)$, HCoO and $CO(NH)_2$ fragment, respectively. Complex **B** gave fragments at m/z = 594, 342, 306, 121, and 58, which correspond to CoL_2H, CoOL, $Co(C_7H_4NO_2)$, C_7H_6NO, and $CO(NH)_2$ fragment, respectively. However, complex **C** underwent fragmentation patterns giving rise to fragments at m/z = 301, 180, and 121 attributed to $Co_2(L)(H_2O)$, $Co_2L(H_2O)C_7H_6NO$ and C_7H_6NO, respectively. All aforementioned spectroscopic tools could confirm and verify the proposed structures of the as-prepared complexes (**A**, B, and **C**) as depicted in Scheme 1.

3.1.2. Thermal analysis

The TGA curves of the as-prepared complexes are shown in Fig. 1(**A**)–(**C**). The thermal decomposition of the complex A ($[CoL(H_2O)_2]_2$), as shown in Fig. 1(Ai), exhibits the presence of two mass loss steps in the temperature range 80–120, and 170–350 °C, corresponding to dehydration of four water molecules and decomposition of the complex **A** to give a residue amounting to cobaltous oxide [28,29] and with a matching mass loss of 11.16 and 63.24% (calculated 10.0 and 67.78%), respectively. However, the percentage of the final residue is 25.6% (calc. 22.22%) corresponding to Co_3O_4 nanoparticles and carbonaceous residue.Fig. 1 (Aii) depicts the DTA analysis for Co_3O_4 showing an endothermic peak at 106 °C, which can be attributed to dehydration of complex **A** and an exothermic peak at 357 °C attributed to the oxidative thermal decomposition of the organic part to leave a final residue of Co_3O_4 oxide and carbon.

According to the TGA analysis, Fig. 1(Bi), complex B ($CoL_2(H_2O)_2$) was thermally decomposed in three steps in the ranges 200–250 and 250–400 °C with a total weight loss of 78.4% leaving cobalt oxide and carbon residues with 12.7%, and 8.9%, respectively. The DTA analysis is shown in Fig. 1(Bii). It exhibited a broad exothermic peak at ca. 380 °C, which was attributed to the decomposition of the organic part of the complex **B** to produce Co_3O_4. The complex **C**, $[Co_2L(H_2O)_8]\cdot 2Cl$, was thermally decomposed as shown in Fig. 1(Ci) in two steps: the first step in the temperature range 80–120 °C with weight loss of 12.2% (calc. 11.7%). This step is associated with the loss of Cl_2, which was consequently accompanied by an endothermic effect on the DTA curve observed at 110 °C, as shown in Fig. 1(Cii). The second step from 250 to 400 °C with weight loss of 61.3% (calc. 61.6%). In this range of temperature, the organic moiety was decomposed and reflected by an intense exothermic effect on DTA curve with a maximum at *ca.* 350 °C. Additionally, the remaining residue of 26.5% (calc. 26.7%) can occur in this step and correspond to tricobalt tetraoxide. Finally, the thermal decomposition steps of **A**, **B** and **C** complexes are formulated in Scheme 2.

3.2. Co_3O_4 nanoparticles

3.2.1. Preparation, morphology and spectral characterization

Fig. 2(A)–(C) displays the XRD patterns of the cobalt oxide nanoparticles obtained by thermal decomposition of the as-prepared complexes (A, B, and C) at 400 °C for 2 h. All of the reflection

- Thermal decomposition of A complex:

1- $[Co_2L_2(H_2O)_4] \xrightarrow{80 - 120\ ^oC} [Co_2L_2] + 4H_2O$

2- $[Co_2L_2] \xrightarrow[-\ n\ H_2O,\ -n\ CO_2]{170 - 350\ ^oC} Co_3O_4 + \text{carbon residue}$

- Thermal decomposition of B complex:

1- $CoL_2(H_2O)_2 \xrightarrow{200 - 250\ ^oC} CoL_2 + 2H_2O$

2- $CoL_2 \xrightarrow[-\ n\ H_2O,\ -n\ CO_2]{250 - 400\ ^oC} Co_3O_4 + \text{carbon residue}$

- Thermal decomposition of C complex:

1- $[Co_2L(H_2O)_8]Cl_2 \xrightarrow{80 - 120\ ^oC} [Co_2L(H_2O)_8] + Cl_2$

2- $[Co_2L(H_2O)_8] \xrightarrow[-\ n\ H_2O,\ -n\ CO_2]{250 - 400\ ^oC} Co_3O_4 + \text{carbon residue}$

Scheme 2. The proposed thermal decomposition pathway of complexes **A**, **B** and **C**.

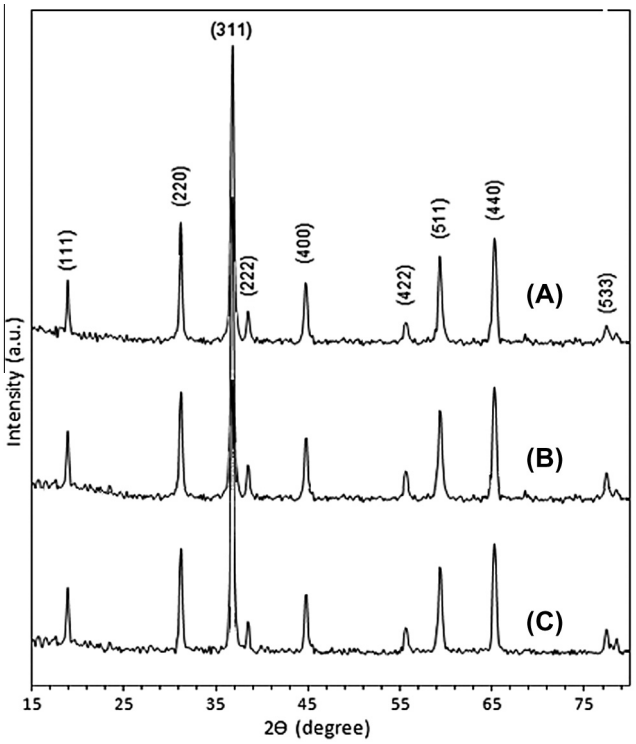

Fig. 2. (A–C) XRD patterns of the Co3O4 nanoparticles (A, B and C) produced by thermal decomposition of A, B and C complexes, respectively.

peaks can be readily indexed to a crystalline cubic Co_3O_4 phase (space group *Fd3m*, lattice constant $a = 8.084$ Å, JCPDS card 74-1657). No other peaks for impurities were detected. The average crystallite size of the Co_3O_4 nanoparticles was calculated using the Scherrer formula (Eq. (1)) [30]:

$$D = 0.89\lambda/\beta\cos\theta_B \quad (1)$$

where λ, β, θ_B are the X-ray wavelength, the full width at half maximum (FWHM) of the diffraction peak and the Bragg diffraction angle, respectively. The estimated average crystallite size of Co_3O_4 nanoparticles was found to be *ca*. 26, 22 and 38 nm, for A-Co_3O_4, B-Co_3O_4, and C-Co_3O_4, respectively.

The infra red spectra of the produced Co_3O_4 samples, as presented in Fig. 3(A)–(C), show two absorption bands at 659 and 562 cm^{-1} which confirm the pure normal spinel structure of Co_3O_4. The first peak is specifically attributed to the stretching vibration mode of ν_{Co-O} in which Co^{2+} is tetrahedrally coordinated, while the band appeared at 562 cm^{-1} can be attributed to the Co–O bond in which Co^{3+} is octahedrally coordinated [31,32].

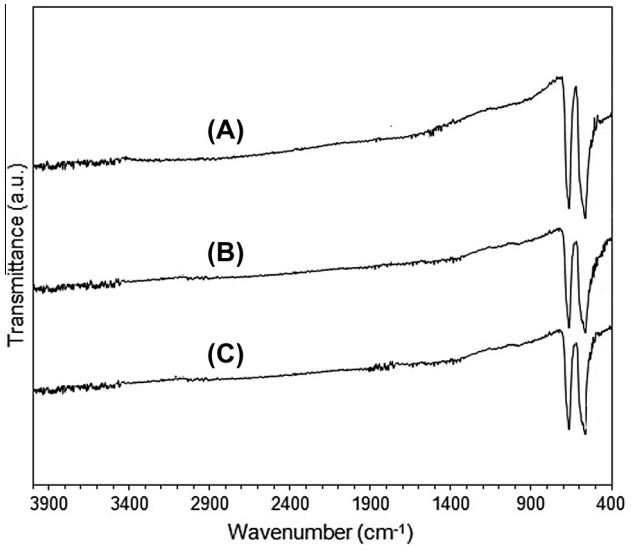

Fig. 3. (A–C) FT-IR spectrum of the produced Co_3O_4 nanoparticles after calcinations at 400 °C in air for 2 h.

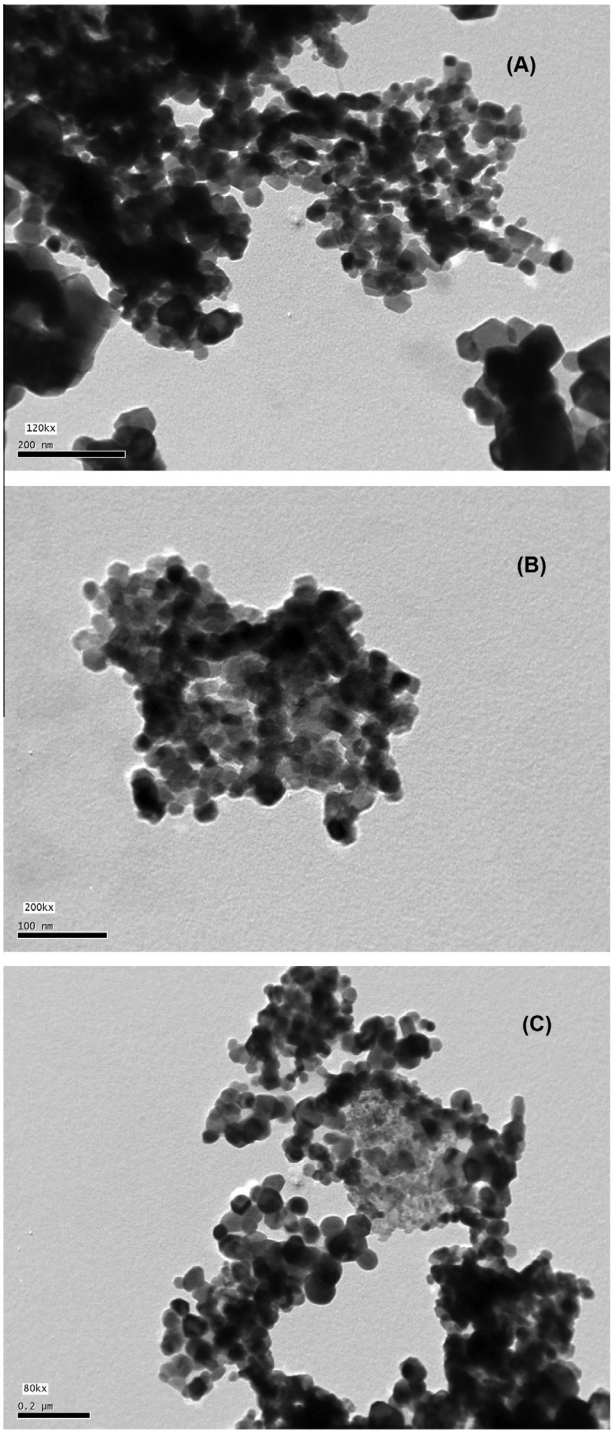

Fig. 4. (A–C) TEM images of the A-, B- and C-Co_3O_4 nanoparticles obtained by thermal decomposition of **A**, **B** and **C** complexes, respectively.

Morphologies of Co_3O_4 nanoparticles, produced by thermal decomposition of the as-prepared complexes, were investigated by TEM as presented in Fig. 4(A)–(C). From the TEM images, it is observed that (A-C)-Co_3O_4 nanoparticles have almost hexagon and square shapes with an average diameter of *ca.* 27, 24 and 40 nm for A-, B- and C-samples, respectively, which is close to the value obtained from the XRD analysis. It can be concluded from the TEM and XRD data that the particle size of the produced cobalt oxide nanoparticles depends on the organic moiety content of the complex undergone thermal decomposition. As the organic moiety content of the complex increased, the particle size of the produced cobalt oxide decreased. Additionally, the organic moiety burned in the thermal decomposition was used as a fuel.

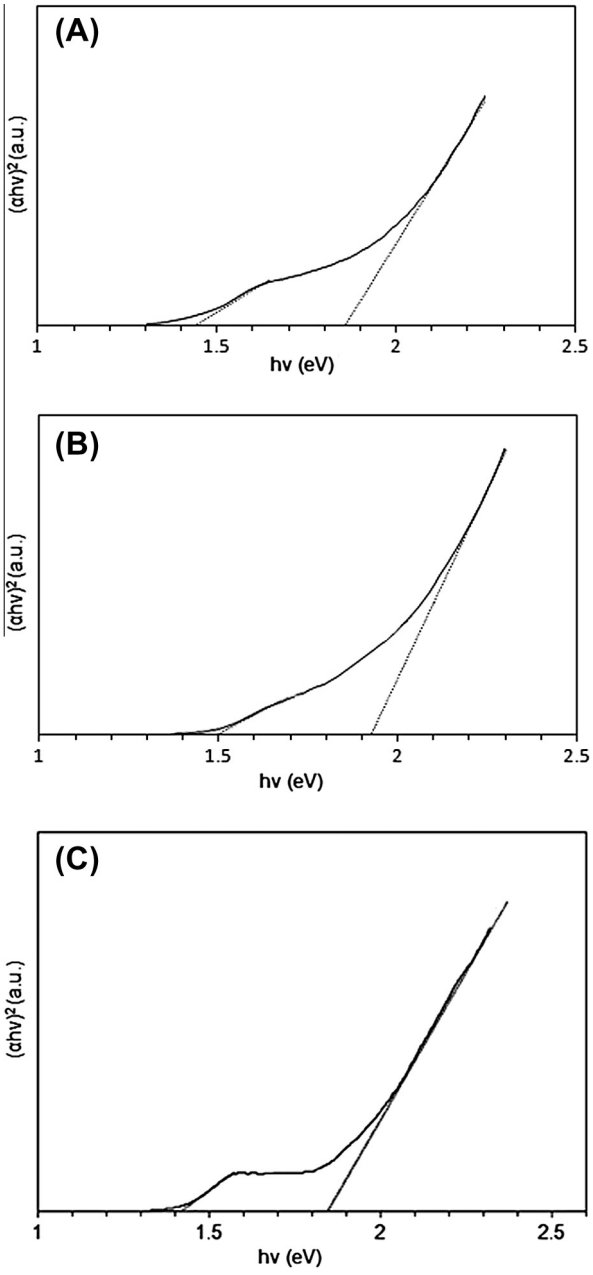

Fig. 5. (A–C) $(\alpha h\nu)^2 \sim h\nu$ curves; A, B and C, for the prepared cobalt oxide samples; A, B and C, respectively.

3.2.2. Optical properties of Co_3O_4 nanoparticles

For pure Co_3O_4, the fundamental UV absorption is due to an inter band transition between the full 2p(O) orbital and the empty 3d(Co^{2+}, Co^{3+}) orbital, which corresponds to what is called the experimental band-gap. The UV absorption spectra of the as-prepared tricobalt tetraoxide samples obtained from different precursors were taken and subsequently the optical band gaps for the spinel cobalt oxides were calculated using the following equation [33,34]:

$$\alpha h\nu = A(h\nu - E_g)^n$$

where α is the linear absorption coefficient, a constant involving properties of the bands, $h\nu$ is the photon energy, A is a constant, E_g is the band gap of the material and the exponent n depends on the type of transition. The values of n for directly allowed, directly forbidden, indirectly allowed, or indirectly forbidden transition are $n = 1/2$, 3/2, 2 and 3, respectively. As shown in Fig. 5(A)–(C), plotting $(\alpha h\nu)^2$ versus $h\nu$ values and then extrapolating the graph to $(\alpha h\nu)^2 = 0$ gave two optical band gaps (E_g), for each cobalt oxide nanoparticles. The obtained band gaps are attributed to the ligand-metal charge transfer transition O(II) → Co(III) and O(II) → Co(II) [9]. The values were found to be (1.48 and 1.86 eV), (1.5 and 1.95 eV) and (1.42, 1.83 eV), for A-, B- and C-cobalt oxide, respectively. It can be concluded that the as-produced cobalt oxides are pure and have semiconducting properties, which are in good agreement with the reported literatures [21,22].

4. Conclusion

Co_3O_4 nanoparticles as normal spinel were produced by thermal decomposition of three novel Co(II)-1,3bis(salicylaldimine) urea complexes as a new metal–organic precursors, at 400 °C for 2 h. These new complexes were solvothermally synthesized using readily available and cheap starting materials such as urea, salicylaldehyde and cobalt chloride at relatively low temperature (120 °C) for 2 h. The as-prepared products were characterized using XRD, magnetism, TEM, FT-IR, TG/DTA analysis, Mass spectrometry and UV–Vis spectroscopy. Moreover, the produced tricobalt tetraoxide showed an optical properties by exhibiting two band gaps in the range of 1.42–1.5 and 1.83–1.95 eV for O(II) → Co(III) and O(II) → Co(II) transitions, respectively.

References

[1] Z.G. Han, Y.Z. Gao, X.L. Zhai, H.H. Song, Inorg. Chem. Commun. 10 (2007) 1079–1082.
[2] J.-P. Sun, L.-C. Li, X.-J. Zheng, Inorg. Chem. Commun. 14 (2011) 877–881.
[3] S. Kotha, Acc. Chem. Res. 36 (2003) 342–351.
[4] M.J. O'Donnell, Acc. Chem. Res. 37 (2004) 506–517.
[5] H.-C. Wu, P. Thanasekaran, C.-H. Tsai, J.-Y. Wu, S.-M. Huang, Y.-S. Wen, K.-L. Lu, Inorg. Chem. 45 (2006) 295–303.
[6] M. Zhao, C. Zhong, C. Stern, A.G.M. Barrett, B.M. Hoffman, J. Am. Chem. Soc. 127 (2005) 9769–9775.
[7] J.L. Sessler, E. Tomat, V.M. Lynch, J. Am. Chem. Soc. 128 (2006) 4184–4185.
[8] S. Das, A. Nag, D. Goswami, P.K. Bharadwaj, J. Am. Chem. Soc. 128 (2006) 402–403.
[9] J. Teichgraber, S. Dechert, F. Meyer, J. Organomet. Chem. 690 (2005) 5255–5263.
[10] M. Veith, A. Altherr, N. Lecerf, Nanostruct. Mater. 12 (1999) 191–194.
[11] X. Nie, Q. Zhao, H. Zheng, J. Cryst. Growth 289 (2006) 299–302.
[12] D. Bayot, M. Degand, M. Devillers, J. Solid State Chem. 178 (2005) 2635–2642.
[13] X.W. Xie, Y. Li, Z.Q. Liu, M. Haruta, W.J. Shen, Nature 458 (2009) 746.
[14] C.H. Chen, S.F. Abbas, A. Morey, S. Sithambaram, L.P. Xu, H.F. Garces, W.A. Hines, S.L. Suib, Adv. Mater. 20 (2008) 1205–1209.
[15] T. He, D. Chen, X. Jiao, Y. Wang, Adv. Mater. 18 (2006) 1078–1082.
[16] H.W. Gu, K.M. Xu, C.J. Xu, B. Xu, Chem. Commun. 9 (2006) 941–949.
[17] X. Wang, X.Y. Chen, L.S. Gao, H.G. Zheng, Z. Zhang, Y.T. Qian, J. Phys. Chem. B 108 (2004) 16401–16404.
[18] R.Z. Yang, Z.X. Wang, J.Y. Liu, L.Q. Chen, Electrochem. Solid State Lett. 7 (2004) A496–A499.
[19] E.L. Salabas, A. Rumplecker, F. Kleitz, F. Radu, F. Schuth, Nano Lett. 6 (2006) 2977–2981.

[20] T. Li, S.G. Yang, L.S. Huang, B.X. Gu, Y.W. Du, Nanotechnology 15 (2004) 1479–1482.
[21] M.Y. Nassar, I.S. Ahmed, Polyhedron 30 (2011) 2431–2437.
[22] M.Y. Nassar, I.S. Ahmed, Mater. Res. Bull. 47 (2012) 2638–2645.
[23] R.L. Carlin, Magnetochemistry, Springer-Verlag, New York, 1986.
[24] G.A. Bain, J.F. Berry, J. Chem. Educ. 85 (2008) 532.
[25] B. Šoptrajanov, V. Stefov, I. Kuzmanovski, G. Jovanovski, H.D. Lutz, B. Engelen, J. Mol. Struct. 613 (2002) 7–14.
[26] K.-L. Zhang, Z. Wang, H. Huang, Y. Zhu, X.-Z. You, J. Mol. Struct. 693 (2004) 193–197.
[27] K. Kurdziel, T. Głowiak, S. Materazzi, J. Jezierska, Polyhedron 22 (2003) 3123–3128.
[28] Z.G. Zhao, F.X. Geng, J.B. Bai, H.M. Cheng, J. Phys. Chem. C 111 (2007) 3848–3852.
[29] A.S. El-Tabl, R.M. Issa, M.A. Morsi, Transit. Met. Chem. 29 (2004) 543–549.
[30] R. Jenkins, R.L. Snyder, Chemical Analysis: Introduction to X-ray Powder Diffractometry, John Wiley and Sons, Inc., New York, 1996.
[31] M. Salavati-Niasari, F. Davar, M. Mazaheri, M. Shaterian, J. Magn. Magn. Mater. 320 (2008) 575–578.
[32] M. Herrero, P. Benito, F.M. Labajos, V. Rives, Catal. Today 128 (2007) 129–137.
[33] M.P. Dare-Edwards, A.H. Goodenough, A. Hammett, P.R. Trevellick, J. Chem. Soc., Faraday Trans. 9 (1983) 2027–2041.
[34] D. Barreca, C. Massignan, S. Daolio, M. Fabrizio, C. Piccirillo, L. Armelao, E. Tondello, Chem. Mater. 13 (2001) 588–593.